Interfacial Vibrational Dynamics of Ice Ihand Liquid Water

Sudera, P.; Cyran, J.D.; Deiseroth, M.; Backus, E.H.G.; Bonn, M.

DOI
10.1021/jacs.0c04526

Publication date
2020

Document Version
Final published version

Published in
Journal of the American Chemical Society

JACS
JOURNAL OF THE AMERICAN CHEMICAL SOCIETY

pubs.acs.org/JACS

Communication

Interfacial Vibrational Dynamics of Ice I_h and Liquid Water

Prerna Sudera, Jenée D. Cyran, Malte Deiseroth, Ellen H. G. Backus,* and Mischa Bonn*

Cite This: *J. Am. Chem. Soc.* 2020, 142, 12005−12009

Read Online

ACCESS | Metrics & More | Article Recommendations | Supporting Information

ABSTRACT: Insights into energy flow dynamics at ice surfaces are essential for understanding chemical dynamics relevant to atmospheric and geographical sciences. Here, employing ultrafast surface-specific spectroscopy, we report the interfacial vibrational dynamics of ice I_h. A comparison to liquid water surfaces reveals accelerated vibrational energy relaxation and dissipation at the ice surface for hydrogen-bonded OH groups. In contrast, free-OH groups sticking into the vapor phase exhibit substantially slower vibrational dynamics on ice. The acceleration and deceleration of vibrational dynamics of these different OH groups at the ice surface are attributed to enhanced intermolecular coupling and reduced rotational mobility, respectively. Our results highlight the unique properties of free-OH groups on ice, putatively linked to the high catalytic activities of ice surfaces.

Solar photon-induced vibrational overtone pumping induces photodissociation of atmospherically relevant compounds[1] like HNO_4,[2] HO_2NO_2,[3] H_2SO_4,[4] etc. When such reagents are adsorbed on omnipresent aqueous or ice surfaces, their vibrational modes can couple to water vibrational modes, e.g., through energy transfer,[5] thereby influencing the reaction pathway. Adsorption on aqueous surfaces can, moreover, shift and intensify OH-stretch overtone absorptions[6] and accelerate photodissociation reactions by orders of magnitude.[7] Besides the potential importance for atmospheric chemistry,[8,9] vibrational energy dynamics on aqueous surfaces are also of fundamental interest for understanding the surface and interfaces[10,11] of arguably the most important molecule on Earth: water.

The vibrational dynamics of interfacial ice have not previously been reported, to the best of our knowledge, owing to the substantial experimental challenge of combining ultrafast surface-sensitive spectroscopy with molecularly defined single-crystalline ice surfaces. Many studies have reported on vibrational dynamics of bulk ice[12−15] and water[16−21] and interfacial water.[11,22−25] Here, we compare the vibrational dynamics of surface OH groups on single-crystalline hexagonal ice (ice I_h) oriented to the basal plane with those on water. OH-oscillators are selectively excited using a femtosecond infrared pulse. The effect of excitation is probed using surface-specific femtosecond sum-frequency generation (SFG) spectroscopy. SFG is a second-order nonlinear process, generally generating signal only from the interfacial molecules. Monitoring the relaxation process of excited oscillators provides information on vibrational lifetimes, heat dissipation, and energy transfer mechanisms.

We study both hydrogen-bonded-OH groups at the surface and free, dangling-OH groups protruding from the surface into the vapor phase. The fraction of interfacial water molecules with a free-OH group is approximately 0.25 for both ice[26] and water.[27] Free-OH groups at the surface of ice are thought to influence chemical reactivities of adsorbates by preferential adsorption,[28] molecular ordering,[29] and energy transfer dynamics.[7,30] We find that, going from water to ice, the vibrational dynamics of hydrogen-bonded-OH groups are accelerated, while those of free-OH groups slow down substantially.

Figure 1a displays the static SFG spectra of water and ice as a function of IR frequency, normalized to the free-OH peak at 3700 cm^{-1}. While the free-OH response is quite similar in its frequency and shape, the hydrogen-bonded region (3000−3600 cm^{-1}) is different. The SFG spectrum of ice in the hydrogen-bonded region is more intense, peaking at ∼3200 cm^{-1}, while the water spectrum is much broader, peaking around ∼3400 cm^{-1}. The spectral red-shift for ice compared to water is indicative of stronger hydrogen bonds in ice.[31] The increased SFG intensity can be explained by the OH-oscillators being more ordered due to the inherent arrangement of water molecules in ice crystals, as opposed to liquid water. This ordering and hence the SFG intensity gets stronger with decreasing temperature. The static ice SFG spectrum shown here is in agreement with previous reports.[32]

In the time-resolved experiments, ice and water surfaces were excited at two frequencies in the hydrogen-bonded region of the OH-stretch band, 3050 and 3310 cm^{-1}, to elucidate if low- or high-frequency excitation affects the surface dynamics, and at the free-OH stretch region, 3700 cm^{-1}, to elucidate the dynamics of the free-OH oscillators on ice (black traces in Figure 1a).

Figure 1b shows the ratio of SFG spectra $I_{SFG}^{exc}/I_{SFG}^{ref}$ as a function of delay time after excitation, with I_{SFG}^{exc} and I_{SFG}^{ref} being the SFG spectrum in the presence and absence of the excitation pulse at 3050 cm^{-1}, respectively. The initial bleach (ratio <1, indicating depopulation of the ground state) around

Received: April 24, 2020
Published: June 23, 2020

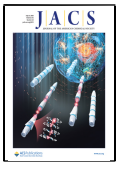

https://dx.doi.org/10.1021/jacs.0c04526
J. Am. Chem. Soc. 2020, 142, 12005−12009

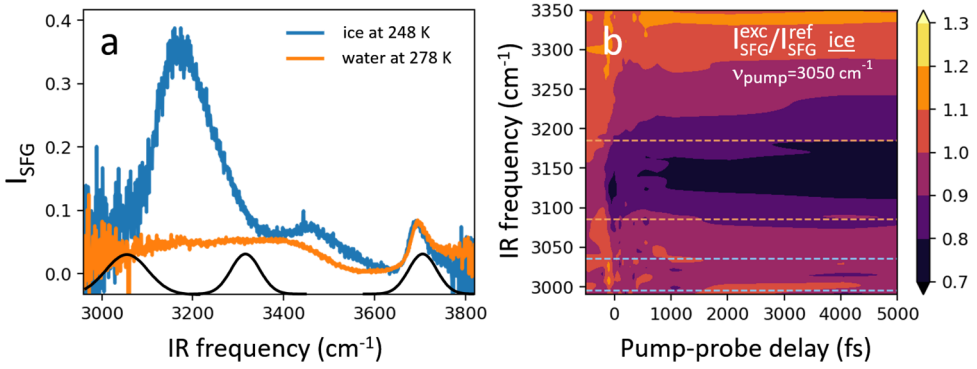

Figure 1. (a) Static SFG spectra of ice and water at 248 and 278 K, respectively, normalized to the free-OH peak around 3700 cm^{-1}. Shown in black are the excitation pulses for the pump−probe measurements centered at 3050, 3310, and 3700 cm^{-1}. (b) Ratio of SFG (SFG$_{exc}$/SFG$_{ref}$) spectra of ice for various delay times, after excitation at 3050 cm^{-1}. Note the initial negative (bleach) signal around 3150 cm^{-1}, accompanied by the positive excited-state SFG signal around 3000 cm^{-1}. The two dashed boxes demarcate the integrated regions for Figure 2a.

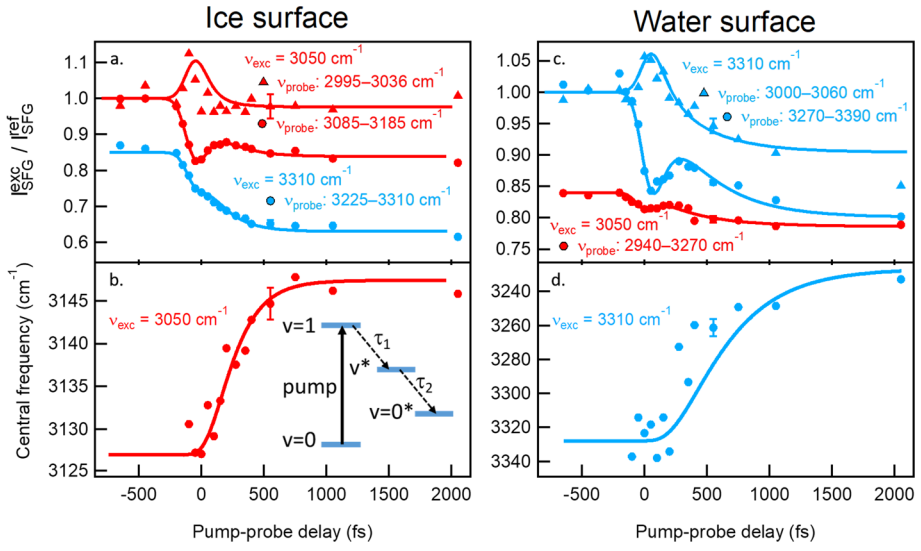

Figure 2. Dynamics traces following vibrational excitation of ice (248 K, panels a, b) and water (278 K, panels c, d) surfaces. Data points in red represent ν_{exc} = 3050 cm^{-1}; in blue, ν_{exc} = 3310 cm^{-1}. Probe frequency range for each system is mentioned in the legends. Circles in panels a and c show probe traces assigned to ground-state-bleach; triangles (ν_{exc} = 3050 cm^{-1} for ice and ν_{exc} = 3310 cm^{-1} for water) show responses assigned to ES SFG. The associated central frequency shift of the SFG response is shown in panels b and d. The data point at 2050 fs in panels b and d is an average of later time points, up to 10 500 fs. Inset in panel b depicts the 4-level model used to describe the traces, represented by solid lines. Traces for ice with ν_{exc} = 3310 cm^{-1} and water with ν_{exc} = 3050 cm^{-1} are offset for clarity. Typical error bars for each plot are shown at 550 fs.

3150 cm^{-1} is spectrally narrow and very short-lived. The bleach is accompanied by an apparent excited state (ES) SFG response from the first vibrationally excited state, represented by the positive signal around 3000 cm^{-1}. Upon decay of the vibrational excitation, there is a relatively slow ingrowth of the signal centered around 3175 cm^{-1}, which reflects the dissipation of excess energy over the system. The Supporting Information (SI) contains data for ice excited at 3310 cm^{-1} and water at both excitation frequencies.

To quantify the dynamics, we integrate data such as that shown in Figure 1b over specific frequency ranges (see SI, Figure S1) to create traces as a function of pump−probe delay, as shown in Figure 2. Panels a and c show traces for ice (248 K) and water (278 K) respectively excited at ν_{exc} = 3050 cm^{-1} (red) and ν_{exc} = 3310 cm^{-1} (blue). The signals integrated close to the respective excitation frequency (filled circles) demonstrate a sharp decrease around time 0, and are assigned to ground state depletion; the recovery is concurrent with heat effects, which appear already within a few 100 fs. These traces marked by circles in panels a and c will hereafter be called ground-state-bleach (GSB) traces. Ice excited at ν_{exc} = 3050 cm^{-1} and water excited at ν_{exc} = 3310 cm^{-1} show, in addition, a transient increase in SFG signal at lower frequencies, represented by triangles in the upper two panels. This signal is assigned to SFG generated from the first excited state, frequency-shifted by the anharmonicity. The ES response for the other excitation frequency could not be detected, probably due to overlap with the bleach and heat signals (see SI). The response at the ES frequency also contains a contribution from the ingrowing heat. Panels b and d show the temporal evolution of the first spectral moment of $I^{exc}_{SFG}/I^{ref}_{SFG}$, obtained from Gaussian fits. These traces highlight relatively slow spectral changes that presumably reflect the ingrowth of heat.

The observed dynamics are modeled (solid lines, Figure2) using the 4-level system, shown in the inset of Figure 2b.[33,34] Excitation occurs from the ground (ν = 0) to the first excited (ν = 1) state. Relaxation with the time constant τ_1 occurs to an intermediate state (ν*, possibly the overtone of the bending

https://dx.doi.org/10.1021/jacs.0c04526
J. Am. Chem. Soc. 2020, 142, 12005−12009

Table 1. Inferred Lifetimes from the 4-Level Model Used to Analyze Vibrational Dynamics, Corresponding to Fitting Lines in Figure 2[a]

	Ice_3050	Water_3050	Ice_3310	Water_3310	Ice_3700	Water_3700
τ_1 (fs)	80 ± 30	60 ± 50	50 ± 30	110 ± 20	2500 ± 600	1150 ± 400
τ_2 (fs)	180 ± 60	380 ± 80	180 ± 60	380 ± 80	–	–

[a]Errors reflect variations between different measurements.

mode[35,36]), from which relaxation to a heated ground state (ν = 0*) occurs with a time constant τ_2. Single-pulse excitation triggers a local temperature rise of a few degrees, weakening the hydrogen bonds,[31] and thereby reducing and blue-shifting the vibrational response[31] (see SI). The 4-level model is well-established to describe the vibrational dynamics of bulk and interfacial water molecules for both liquid water and ice.[33,34,37] Using the model, we disentangle heat effects from the relaxation process and extract the two time constants.

For each of the four data sets (ice and water pumped at ν_{exc} = 3050 and 3310 cm^{-1}), the respective GSB, ES response, and thermal effects (Figure 2b,d) are described using the same set of parameters, τ_1 and τ_2. Specifically, the GSB trace includes the population difference between ν = 0 and ν = 1, and the populations of ν* and ν = 0*. The ES trace includes ν = 1 with a contribution from ν = 0* (heat). Since the shift of the central frequency (Figure 2b,d) reflects heating, it is modeled with the population of ν = 0* (heat). τ_2 was fitted globally to all data sets, for ice (180 fs) and water (380 fs). τ_1 was allowed to vary with excitation frequency (for details, see SI). Given these constraints, the model describes the data well (lines in Figure 2). Table 1 shows the inferred time constants. The dynamics for the hydrogen-bonded region appear, on average, faster for ice than for water, which can be attributed to stronger intermolecular coupling effects in ice.[12] τ_1 is a measure of the energy relaxation time of the excited oscillators but will also include spectral diffusion. Within experimental uncertainty, we find no evidence for a frequency dependence of τ_1 for ice, implying relative homogeneity of the hydrogen-bonded OH groups for ice. τ_2 for ice is substantially faster than for water, illustrating highly efficient heat dissipation. Interestingly, τ_2 for interfacial water is very similar to that observed for bulk,[24,34] yet τ_2 for interfacial ice is substantially faster than the ~500 fs reported for bulk ice.[13]

Figure 3 shows the vibrational dynamics of the free-OH stretch (spectral feature at ~3700 cm^{-1} in Figure 1a) at both water (replotted from ref 38) and ice surfaces. Ice was pumped at ~3680 cm^{-1} and probed from 3675 to 3705 cm^{-1}. The free-OH groups are less sensitive to heat effects, owing to the vanishingly small absorption in bulk at this frequency.[39] A simple single-exponential decay convoluted with the instrument response function describes the data well (solid lines in Figure 3 and Table 1 for the time scales).

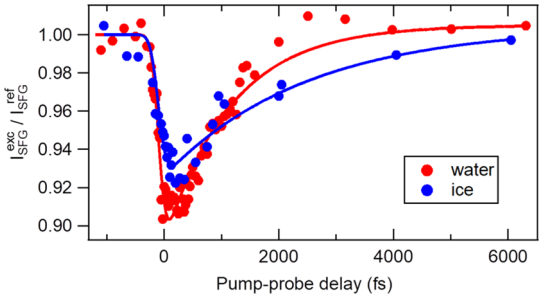

Figure 3. Vibrational dynamics at the free-OH frequency. Traces were obtained by exciting and probing the ice (blue) and water (red) surfaces at 3700 cm^{-1}. Lines are single-exponential decays convoluted with the instrument response function.

As apparent from the data, the vibrational relaxation of free-OH groups protruding from ice is substantially slower than for water. At first sight, this may appear surprising, given the accelerated vibrational dynamics for ice in the hydrogen-bonded region. The vibrational relaxation of the free-OH groups protruding from liquid water has been shown to take place via the combination of two mechanisms:[38,40] (i) the reorientation of water molecules containing free-OH groups, so that these become hydrogen-bonded, and (ii) intramolecular energy transfer (IET) from the free-OH group to the other OH group in the same water molecule. In both cases, the excitation disappears from the free-OH group.[22,38] Since water molecules in ice form a more rigid structural arrangement compared to those in liquid water, the first mechanism involving reorientation of the water molecule is expected to be suppressed for ice. IET in ice should also slow down, owing to the larger frequency mismatch between the free-OH and the hydrogen-bonded-OH within the same molecule for ice[26] (3690 to 3350 cm^{-1}) compared to water[41] (3700 to 3510 cm^{-1}). The suppression of reorientation due to structural rigidity and slow-down of IET result in substantially slower free-OH dynamics for ice.

In conclusion, we have reported ultrafast vibrational dynamics of the ice interface. This study paves the way to time-resolved studies using optical or UV excitation to initiate surface photochemistry and follow the subsequent dynamics in real-time. The vibrational dynamics of water molecules at the surface of ice are faster or slower compared to those in liquid water, depending on whether the hydrogen-bonded- or dangling-OH groups are considered. The ordered crystalline arrangement of water molecules in ice promotes strong inter- and intramolecular coupling, making energy transfer in the bonded-OH stretch region extremely fast. This efficient energy transport from the bonded-OH groups into the bulk ice crystal is potentially relevant for the dissipation of adsorbed (OH-bonded) reactants at the ice surface. In contrast, the dangling-OH shows much slower dynamics for ice compared to liquid water, due to the structural rigidity of ice. The long vibrational lifetime of free-OH groups reflects their long physical lifetime, offering a potential explanation for kinetic trapping mechanisms[42] on the surface of ice, and for the isolation of reaction intermediates and preferential stabilization of charged species on the surface.[43] Differences in binding mechanism[28] and vibrational relaxation rates may account for differences in photochemical reactions on the surfaces of ice and water.[44,45]

■ ASSOCIATED CONTENT

Supporting Information

The Supporting Information is available free of charge at https://pubs.acs.org/doi/10.1021/jacs.0c04526.

https://dx.doi.org/10.1021/jacs.0c04526
J. Am. Chem. Soc. 2020, 142, 12005−12009

Additional data, blue- vs red-shifting of spectra, model, and methods (PDF)

AUTHOR INFORMATION

Corresponding Authors

Ellen H. G. Backus − *Max Planck Institute for Polymer Research, 55128 Mainz, Germany; University of Vienna, 1090 Vienna, Austria;* orcid.org/0000-0002-6202-0280; Email: ellen.backus@univie.ac.at

Mischa Bonn − *Max Planck Institute for Polymer Research, 55128 Mainz, Germany;* orcid.org/0000-0001-6851-8453; Email: bonn@mpip-mainz.mpg.de

Authors

Prerna Sudera − *Max Planck Institute for Polymer Research, 55128 Mainz, Germany*

Jenée D. Cyran − *Max Planck Institute for Polymer Research, 55128 Mainz, Germany; Baylor University, Waco, Texas 76798, United States;* orcid.org/0000-0002-5278-9854

Malte Deiseroth − *Max Planck Institute for Polymer Research, 55128 Mainz, Germany*

Complete contact information is available at: https://pubs.acs.org/10.1021/jacs.0c04526

Notes

The authors declare no competing financial interest.

ACKNOWLEDGMENTS

We thank Marc-Jan van Zadel, Hansjörg Menges, and Florian Gericke for excellent technical support, and Johannes Hunger and Yuki Nagata for helpful discussions. We are grateful for financial support from the MaxWater initiative from the Max Planck Society.

REFERENCES

(1) Donaldson, D. J.; Tuck, A. F.; Vaida, V. Atmospheric Photochemistry via Vibrational Overtone Absorption. *Chem. Rev.* **2003**, *103* (12), 4717−4730.

(2) Donaldson, D. J.; Frost, G. J.; Rosenlof, K. H.; Tuck, A. F.; Vaida, V. Atmospheric Radical Production by Excitation of Vibrational Overtones via Absorption of Visible Light. *Geophys. Res. Lett.* **1997**, *24* (21), 2651−2654.

(3) Staikova, M.; Donaldson, D. J.; Francisco, J. S. Overtone-Induced Reactions on the HO2NO2 Potential Surface. *J. Phys. Chem. A* **2002**, *106* (12), 3023−3028.

(4) Vaida, V. Photolysis of Sulfuric Acid Vapor by Visible Solar Radiation. *Science* **2003**, *299* (5612), 1566−1568.

(5) Shin, H. K. Inter- and Intramolecular Vibrational Energy Flow in a Formamide−Water Complex. *J. Phys. Chem. A* **2020**, *124* (16), 3031−3037.

(6) Staikova, M.; Donaldson, D. J. Water Complexes as Catalysts in Atmospheric Reactions. *Phys. Chem. Earth, Part C Solar, Terr. Planet. Sci.* **2001**, *26* (7), 473−478.

(7) Staikova, M.; Oh, M.; Donaldson, D. J. Overtone-Induced Decarboxylation: A Potential Sink for Atmospheric Diacids. *J. Phys. Chem. A* **2005**, *109* (4), 597−602.

(8) Devlin, J. P.; Uras, N.; Sadlej, J.; Buch, V. Discrete Stages in the Solvation and Ionization of Hydrogen Chloride Adsorbed on Ice Particles. *Nature* **2002**, *417* (6886), 269−271.

(9) Tolbert, M. A.; Rossi, M. J.; Golden, D. M. Antarctic Ozone Depletion Chemistry: Reactions of N2O5 with H2O and HCl on Ice Surfaces. *Science* **1988**, *240* (4855), 1018−1021.

(10) Cyran, J. D.; Backus, E. H. G.; Nagata, Y.; Bonn, M. Structure from Dynamics: Vibrational Dynamics of Interfacial Water as a Probe of Aqueous Heterogeneity. *J. Phys. Chem. B* **2018**, *122* (14), 3667−3679.

(11) Nihonyanagi, S.; Yamaguchi, S.; Tahara, T. Ultrafast Dynamics at Water Interfaces Studied by Vibrational Sum Frequency Generation Spectroscopy. *Chem. Rev.* **2017**, *117* (16), 10665−10693.

(12) Timmer, R. L. A.; Bakker, H. J. Vibrational Förster Transfer in Ice Ih. *J. Phys. Chem. A* **2010**, *114* (12), 4148−4155.

(13) Perakis, F.; Hamm, P. Two-Dimensional Infrared Spectroscopy of Neat Ice Ih. *Phys. Chem. Chem. Phys.* **2012**, *14* (18), 6250−6256.

(14) Dokter, A. M.; Bakker, H. J. Transient Absorption of Vibrationally Excited Ice Ih. *J. Chem. Phys.* **2008**, *128* (2), No. 024502.

(15) Woutersen, S.; Emmerichs, U.; Nienhuys, H. K.; Bakker, H. J. Anomalous Temperature Dependence of Vibrational Lifetimes in Water and Ice. *Phys. Rev. Lett.* **1998**, *81* (5), 1106−1109.

(16) Cowan, M. L.; Bruner, B. D.; Huse, N.; Dwyer, J. R.; Chugh, B.; Nibbering, E. T. J.; Elsaesser, T.; Miller, R. J. D. Ultrafast Memory Loss and Energy Redistribution in the Hydrogen Bond Network of Liquid H2O. *Nature* **2005**, *434* (7030), 199−202.

(17) Roberts, S. T.; Ramasesha, K.; Tokmakoff, A. Structural Rearrangements in Water Viewed through Two-Dimensional Infrared Spectroscopy. *Acc. Chem. Res.* **2009**, *42* (9), 1239−1249.

(18) Woutersen, S.; Bakker, H. J. Resonant Intermolecular Transfer of Vibrational Energy in Liquid Water. *Nature* **1999**, *402* (6761), 507−509.

(19) Nibbering, E. T. J.; Elsaesser, T. Ultrafast Vibrational Dynamics of Hydrogen Bonds in the Condensed Phase. *Chem. Rev.* **2004**, *104* (4), 1887−1914.

(20) Pakoulev, A.; Wang, Z.; Dlott, D. D. Vibrational Relaxation and Spectral Evolution Following Ultrafast OH Stretch Excitation of Water. *Chem. Phys. Lett.* **2003**, *371* (5−6), 594−600.

(21) Stenger, J.; Madsen, D.; Dreyer, J.; Nibbering, E. T. J.; Hamm, P.; Elsaesser, T. Coherent Response of Hydrogen Bonds in Liquids Probed by Ultrafast Vibrational Spectroscopy. *J. Phys. Chem. A* **2001**, *105* (13), 2929−2932.

(22) Hsieh, C.-S.; Okuno, M.; Hunger, J.; Backus, E. H. G.; Nagata, Y.; Bonn, M. Aqueous Heterogeneity at the Air/Water Interface Revealed by 2D-HD-SFG Spectroscopy. *Angew. Chem., Int. Ed.* **2014**, *53* (31), 8146−8149.

(23) Zhang, Z.; Piatkowski, L.; Bakker, H. J.; Bonn, M. Ultrafast Vibrational Energy Transfer at the Water/Air Interface Revealed by Two-Dimensional Surface Vibrational Spectroscopy. *Nat. Chem.* **2011**, *3* (11), 888−893.

(24) McGuire; Shen. Ultrafast Vibrational Dynamics at Water Interfaces. *Science* **2006**, *313* (5795), 1945−1948.

(25) Smits, M.; Ghosh, A.; Sterrer, M.; Müller, M.; Bonn, M. Ultrafast Vibrational Energy Transfer between Surface and Bulk Water at the Air-Water Interface. *Phys. Rev. Lett.* **2007**, *98* (9), No. 098302.

(26) Smit, W. J.; Tang, F.; Sánchez, M. A.; Backus, E. H. G.; Xu, L.; Hasegawa, T.; Bonn, M.; Bakker, H. J.; Nagata, Y. Excess Hydrogen Bond at the Ice-Vapor Interface around 200 K. *Phys. Rev. Lett.* **2017**, *119* (13), 133003.

(27) Du, Q.; Freysz, E.; Shen, Y. R. Surface Vibrational Spectroscopic Studies of Hydrogen Bonding and Hydrophobicity. *Science* **1994**, *264* (5160), 826−828.

(28) Cyran, J. D.; Backus, E. H. G.; van Zadel, M.-J.; Bonn, M. Comparative Adsorption of Acetone on Water and Ice Surfaces. *Angew. Chem., Int. Ed.* **2019**, *58* (11), 3620−3624.

(29) Buch, V.; Groenzin, H.; Li, I.; Shultz, M. J.; Tosatti, E. Proton Order in the Ice Crystal Surface. *Proc. Natl. Acad. Sci. U. S. A.* **2008**, *105* (16), 5969−5974.

(30) Kato, F.; Sugimoto, T.; Matsumoto, Y. Direct Experimental Evidence for Markedly Enhanced Surface Proton Activity Inherent to Water Ice. *J. Phys. Chem. Lett.* **2020**, *11* (7), 2524−2529.

(31) Novak, A. Hydrogen Bonding in Solids Correlation of Spectroscopic and Crystallographic Data. *Large Molecules*; Structure and Bonding Vol. 18; Springer: Berlin, Heidelberg, 1974; pp 177−216. DOI: 10.1007/BFb0116438.

(32) Sánchez, M. A.; Kling, T.; Ishiyama, T.; van Zadel, M.-J.; Bisson, P. J.; Mezger, M.; Jochum, M. N.; Cyran, J. D.; Smit, W. J.; Bakker, H. J.; Shultz, M. J.; Morita, A.; Donadio, D.; Nagata, Y.; Bonn, M.; Backus, E. H. G. Experimental and Theoretical Evidence for Bilayer-by-Bilayer Surface Melting of Crystalline Ice. *Proc. Natl. Acad. Sci. U. S. A.* **2017**, *114* (2), 227−232.
(33) Deiseroth, M.; Bonn, M.; Backus, E. H. G. Electrolytes Change the Interfacial Water Structure but Not the Vibrational Dynamics. *J. Phys. Chem. B* **2019**, *123* (40), 8610−8616.
(34) Lock, A. J.; Woutersen, S.; Bakker, H. J. Ultrafast Energy Equilibration in Hydrogen-Bonded Liquids. *J. Phys. Chem. A* **2001**, *105* (8), 1238−1243.
(35) Deàk, J. C.; Rhea, S. T.; Iwaki, L. K.; Dlott, D. D. Vibrational Energy Relaxation and Spectral Diffusion in Water and Deuterated Water. *J. Phys. Chem. A* **2000**, *104* (21), 4866−4875.
(36) Finzi, J. Vibrational Relaxation of Water Vapor. *J. Chem. Phys.* **1999**, *67* (9), 4053.
(37) Nienhuys, H. K.; Woutersen, S.; Van Santen, R. A.; Bakker, H. J. Mechanism for Vibrational Relaxation in Water Investigated by Femtosecond Infrared Spectroscopy. *J. Chem. Phys.* **1999**, *111* (4), 1494−1500.
(38) Hsieh, C.-S.; Campen, R. K.; Okuno, M.; Backus, E. H. G.; Nagata, Y.; Bonn, M. Mechanism of Vibrational Energy Dissipation of Free OH Groups at the Air-Water Interface. *Proc. Natl. Acad. Sci. U. S. A.* **2013**, *110* (47), 18780−18785.
(39) Clapp, M. L.; Worsnop, D. R.; Miller, R. E. Frequency-Dependent Optical Constants of Water Ice Obtained Directly from Aerosol Extinction Spectra. *J. Phys. Chem.* **1995**, *99* (17), 6317−6326.
(40) Xiao, S.; Figge, F.; Stirnemann, G.; Laage, D.; McGuire, J. A. Orientational Dynamics of Water at an Extended Hydrophobic Interface. *J. Am. Chem. Soc.* **2016**, *138* (17), 5551−5560.
(41) Stiopkin, I. V.; Weeraman, C.; Pieniazek, P. A.; Shalhout, F. Y.; Skinner, J. L.; Benderskii, A. V. Hydrogen Bonding at the Water Surface Revealed by Isotopic Dilution Spectroscopy. *Nature* **2011**, *474* (7350), 192−195.
(42) Kang, H. Chemistry of Ice Surfaces. Elementary Reaction Steps on Ice Studied by Reactive Ion Scattering. *Acc. Acc. Chem. Res.* **2005**, *38* (12), 893−900.
(43) Jung, K.-H.; Park, S.-C.; Kim, J.-H.; Kang, H. Vertical Diffusion of Water Molecules near the Surface of Ice. *J. Chem. Phys.* **2004**, *121*, 2758.
(44) Kahan, T. F.; Donaldson, D. J. Photolysis of Polycyclic Aromatic Hydrocarbons on Water and Ice Surfaces. *J. Phys. Chem. A* **2007**, *111* (7), 1277−1285.
(45) Kahan, T. F.; Zhao, R.; Jumaa, K. B.; Donaldson, D. J. Anthracene Photolysis in Aqueous Solution and Ice: Photon Flux Dependence and Comparison of Kinetics in Bulk Ice and at the Air−Ice Interface. *Environ. Sci. Technol.* **2010**, *44* (4), 1302−1306.

https://dx.doi.org/10.1021/jacs.0c04526
J. Am. Chem. Soc. 2020, 142, 12005−12009